Exposure-response analysis of alemtuzumab in pediatric allogeneic HSCT for nonmalignant diseases: the ARTIC study

Achini-Gutzwiller, F.R.; Schilham, M.W.; Asmuth, E.G.J. von; Jansen-Hoogendijk, A.M.; Zijde, C.M. van der; Tol, M.J.D. van; ... ; Moes, D.J.A.R.

REGULAR ARTICLE

blood advances

Exposure-response analysis of alemtuzumab in pediatric allogeneic HSCT for nonmalignant diseases: the ARTIC study

Federica R. Achini-Gutzwiller,[1-3] Marco W. Schilham,[2] Erik G. J. von Asmuth,[2] Anja M. Jansen-Hoogendijk,[2] Cornelia M. Jol-van der Zijde,[2] Maarten J. D. van Tol,[2] Robbert G. M. Bredius,[3] Tayfun Güngör,[1,*] Arjan C. Lankester,[3,*] and Dirk Jan A. R. Moes[4,*]

[1]Department of Pediatric Stem Cell Transplantation and Hematology, Children's Research Center, University Children's Hospital Zurich, Zurich, Switzerland; and [2]Laboratory for Pediatric Immunology, [3]Department of Pediatric Stem Cell Transplantation, Willem-Alexander Children's Hospital, and [4]Department of Clinical Pharmacy and Toxicology, Leiden University Medical Center, Leiden, The Netherlands

Key Points

- An alemtuzumab population pharmacokinetic model has been developed for more accurate intravenous dosing in pediatric HSCT.
- Optimal exposure is associated with early T-cell recovery and prevention of graft failure.

Alemtuzumab (anti-CD52 antibody) is frequently prescribed to children with nonmalignant diseases undergoing allogeneic hematopoietic stem cell transplantation (HSCT) to prevent graft failure (GF) and acute graft-versus-host disease (aGVHD). The aim of this multicenter study was the characterization of alemtuzumab population pharmacokinetics to perform a novel model–based exposure-response analysis in 53 children with nonmalignant immunological or hematological disease and a median age of 4.4 years (interquartile range [IQR], 0.8-8.7). The median cumulative alemtuzumab dose was 0.6 mg/kg (IQR, 0.6-1) administered over 2 to 7 days. A 2-compartment population pharmacokinetics model with parallel linear and nonlinear elimination including allometrically scaled bodyweight (median, 17.50 kg; IQR, 8.76-33.00) and lymphocyte count at baseline (mean, 2.24×10^9/L; standard deviation ± 1.87) as significant pharmacokinetic predictors was developed using nonlinear mixed effects modeling. Based on the model–estimated median concentration at day of HSCT (0.77 μg/mL; IQR, 0.33-1.82), patients were grouped into a low- (≤0.77 μg/mL) or high- (>0.77 μg/mL) exposure groups. High alemtuzumab exposure at day of HSCT correlated with delayed $CD4^+$ and $CD8^+$ T-cell reconstitution (*P* value < .0001) and increased risk of GF (*P* value = .043). In contrast, alemtuzumab exposure did not significantly influence the incidence of aGVHD grade ≥2, mortality, chimerism at 1 year, viral reactivations, and autoimmunity at a median follow-up of 3.3 years (IQR, 2.5-8.0). In conclusion, this novel population pharmacokinetics model is suitable for individualized intravenous precision dosing to predict alemtuzumab exposure in pediatric allogeneic HSCT for nonmalignant diseases, aiming at the achievement of early T-cell reconstitution and prevention of GF in future prospective studies.

Introduction

For many children with inherited immune or hematological disorders, allogeneic hematopoietic stem cell transplantation (HSCT) is the only established curative treatment. However, transplant-related morbidity

Submitted 29 September 2022; accepted 20 May 2023; prepublished online on *Blood Advances* First Edition 7 June 2023; final version published online 11 August 2023. https://doi.org/10.1182/bloodadvances.2022009051.

*T.G., A.C.L., and D.J.A.R.M. contributed equally to this study.

Data that support the findings of this study are available in the electronic supplementary material of this article. Further information on the pharmacokinetic model development and on data analysis may be found in a data supplement available with the online version of this article. Original pharmacokinetic data are available upon request from the corresponding author, Federica R. Achini-Gutzwiller (Federica.achini@kispi.uzh.ch).

The full-text version of this article contains a data supplement.

and mortality due to graft failure (GF), acute graft-versus-host disease (aGVHD) and late T-cell recovery remain serious complications. Alemtuzumab is widely used as part of conditioning regimens to induce profound immunosuppression, thereby preventing these alloimmune complications.[1-3]

Alemtuzumab (Campath-1H) is a humanized monoclonal immunoglobulin G1 antibody with a rat-derived antigen-specific Fab region and a human Fc region.[1,4] This antibody targets the human CD52 antigen, a membrane protein highly expressed on the surface of T and B lymphocytes and at a lower level on monocytes, macrophages, natural killer (NK) cells, and neutrophils but not on hematopoietic stem cells.[5,6] In vivo studies indicated antibody-dependent cell-mediated cytotoxicity, mainly mediated by neutrophils and NK cells, as the key mechanism of alemtuzumab action.[7-12] The impact of alemtuzumab on immune depletion in the extravascular compartment is still largely unknown and might be limited.[5,8,13,14]

Although alemtuzumab has been demonstrated to contribute to improve clinical outcome after HSCT,[15-17] its efficacy may be limited by the long half-time of 15 to 21 days[18] and large in vivo interindividual pharmacokinetic (PK) variability, possibly leading to unintended overdosing and unfavorable delayed immune reconstitution.[19,20] Current pediatric recommendations for intravenous administration are based on clinical practice and bodyweight (0.5-1.0 mg/kg intravenously) rather than on PK.[21] Overall, published data on pediatric alemtuzumab population PKs are limited to subcutaneous administration[22] or to a single study addressing intravenous drug administration.[21] Available data on intravenous alemtuzumab administration present further important limitations such as its retrospective nature, the infrequent amount of standardized PK measurements per patient, its collection from a mixed cohort of malignant/nonmalignant diseases, and patient recruitment after all HSCT procedures. In addition, a large amount of the very high interindividual PK variability could not be explained. Individualized treatment guided by model-informed precision dosing could significantly decrease interpatient variability in alemtuzumab exposure and potentially lead to more favorable clinical outcomes.

Here, we report a combined prospective and retrospective multicenter PK study on intravenously administered alemtuzumab in children undergoing HSCT for nonmalignant diseases, which resulted in the development of a reliable population PK model and allowed for analysis of the correlation between alemtuzumab exposure and clinical and immunological outcome parameters after transplantation.

Methods

Study design, participants, and donors

The impact of alemtuzumab exposure on immune reconstitution, autoimmunity, risk of infection, chimerism and GVHD in children with nonmalignant diseases undergoing allogeneic SCT (ARTIC) study was conducted between 2019 and 2021 at the University Children's Hospital Zurich, Switzerland, and at the Willem Alexander Children's Hospital, Leiden University Medical Center, The Netherlands, as an international multicenter observational trial. Children and adolescents aged ≤18 years, diagnosed with severe inborn errors of immunity or severe nonmalignant hematological disorders with an indication for a first HSCT have been recruited. All patients who received transplantation between 2010 and 2019 for whom serum samples were available were retrospectively enrolled. Patients who received prior alemtuzumab were not eligible to participate in this study. Donors were selected based on high-resolution HLA-typing per current guidelines.[2] GVHD prophylaxis and supportive care were given following local institutional guidelines. Institutional ethical committee approval was obtained for this trial, which was registered in both the Swiss (BASEC-2018-00794) and Dutch (NTR, NL-8185) registry and conducted in compliance with the Declaration of Helsinki.

Alemtuzumab treatment, sampling, and analysis

Alemtuzumab (Campath-1H, Sanofi Genzyme, Cambridge, MA) was administered intravenously in at least 2 infusions of 4 to 12 hours each at a total dose of 0.2 to 1.5 mg/kg bodyweight as part of the respective conditioning regimen in line with institutional and European Society for Blood and Marrow Transplantation–Inborn Errors Working Party guidelines (electronic supplemental Material; supplemental Figure 1).[2,21] For evaluation of alemtuzumab PKs, all previously collected and cryopreserved serum samples from the first-dose administration until 6 weeks after transplantation were retrospectively analyzed for alemtuzumab concentration. In the prospectively recruited patient group, serum samples were collected for PK analysis before and after each alemtuzumab infusion, at day of HSCT and at least once per week over a 6-week period after HSCT. Patient samples were stored at −80°C until analysis.

Alemtuzumab concentrations were determined with a sensitive (lower limit of quantification, 0.0005 μg/mL) sandwich enzyme-linked immunosorbent assay as previously described by our group.[23]

Population PK modeling

The primary aim of this study was to characterize the population PK of alemtuzumab after intravenous administration in this pediatric cohort for subsequent exposure-response analysis. Based on the obtained alemtuzumab concentration-time data, a nonlinear mixed-effects model (NONMEM, version 7.4.4; Icon Development Solutions, Ellicott City, MD) was developed to define the PK characteristics of alemtuzumab in this patient population.[24,25] A first-order conditional estimation with interaction approach was used and both 1- and 2-compartmental models with linear or parallel linear and nonlinear elimination were explored. Candidate models were evaluated based on the provided objective function value (OFV), calculated as the −2-log likelihood. A change of OFV between candidate structural models is assumed to follow a χ^2 distribution (1 degree of freedom) and a decrease in OFV of ≥6.63 was considered statistically significant ($P < .01$).

A full population PK covariate analysis was performed in which the influence of demographic data, transplant characteristics, and laboratory parameters just before the infusion of the first alemtuzumab dose (obtained from the electronic health care record) were tested (electronic supplemental Material; supplemental Table 1). The predictive performance of the final model was evaluated with a prediction-corrected visual predictive check, which was based on 1000 Monte Carlo simulations.[26] The precision of the model parameter estimates was evaluated by means of a nonparametric bootstrap resampling the data set, 1000-fold. Pirana was used as

modeling environment (version 2.9.8).[27] R Studio (version 2021.9.0.351) and R statistics (version 4.1.2) were used for both exploratory graphical analysis as well as for evaluation of the model's goodness of fit (GOF), prediction-corrected visual predictive check, and outcome analysis, as described hereafter.[28,29]

Model–estimated individual PK parameters of drug clearance (CL), volume of distribution (Vd), maximum elimination rate, and concentration at which the elimination pathway is half saturated were estimated and used to calculate 5 different PK exposure metrics: day until which alemtuzumab level reached its estimated lympholytic level of <0.1 μg/mL, alemtuzumab level (μg/mL) at HSCT day, cumulative area under the curve ($AUC_{0-\infty}$, μg/mL per day), AUC until HSCT, and AUC after HSCT.

Sample size calculation

Our analysis addressed GF, defined as nonengraftment or poor graft performance leading to a second HSCT procedure, and further clinical and immunological end points. The initial target sample size was 30 patients based on the scarce overall incidence of severe immunological and hematological disorders,[15,30] but accrual was expanded to 50 patients after interim analysis, which revealed an incidence of GF of 20% (6/30). Accounting for the incidence of GF in a pediatric cohort with comparable diseases (58.8%, 20/34),[31,32] power analysis based on a 2-sample proportion test for noninferiority with a power of 90%, an α-error of 5%, a noninferiority margin of 85%, and a dropout rate of 2.5%, resulted in a sample size of 50 patients.

Outcome parameters

The primary end point of this study was the assessment of an exposure-response correlation between alemtuzumab exposure and the incidence of GF.

The secondary end point was the assessment of an exposure-response correlation between alemtuzumab exposure and relevant outcome parameters such as the reconstitution of the immune system, which was routinely assessed at least monthly after HSCT. An absolute $CD4^+$ T-cell count of $\geq 0.05 \times 10^9$/L on 2 consecutive measurements was used to define the time point of cell recovery. There is no established absolute cell count defining the recovery of $CD8^+$ T cells, B cells, and NK cells after HSCT. In this study, we decided to arbitrarily use the same value as for the analysis of $CD4^+$ T cells ($\geq 0.05 \times 10^9$/L) on 2 consecutive measurements. Although neutrophil engraftment was defined as an absolute neutrophil count of at least 0.5×10^9/L, monocyte recovery was achieved at an absolute cell count of $\geq 0.1 \times 10^9$/L. Additional parameters analyzed were the incidence and grade of acute and chronic GVHD, the incidence of mortality, and mixed donor chimerism at 1-year after transplantation, defined as <95% donor cells in peripheral blood mononucleated cells. Acute and chronic GVHD were graded per the classic Glucksberg-Seattle scale and the National Institutes of Health criteria, respectively.[33] We further considered the incidence of cytomegalovirus (CMV), Epstein-Barr virus, and adenovirus reactivations, defined as 1 polymerase chain reaction measurement >3 $\log_{10}$ copies per mL, and the incidence of hematological and nonhematological autoimmune complications.

Statistics

Duration of follow-up was defined as the time from HSCT to the last follow-up or death. Patients were censored because of loss to follow-up or study withdrawal. The association between potential predictor variables such as demographic data, diagnosis category (immunological vs hematological diagnosis), and transplant characteristics (intensity of conditioning regimen, donor type, and graft source) with alemtuzumab exposure was tested univariately, using the Wilcoxon signed rank test to compare medians of continuous variables, and the Fisher exact test to compare frequencies of categorical variables. Although concomitant events may have a relevant impact on the occurrence of other outcomes of interest (eg, occurrence of aGVHD and risk of mixed chimerism), they were not included in univariate analysis to avoid reverse causality bias. Immune cell engraftment and reconstitution were analyzed by Kaplan-Meier, and tested univariately using a log-rank test. Other time-to-event outcomes were tested using competing risk analysis, with death as a competing risk for all outcomes except overall survival, and second HSCT as a competing risk for all outcomes except second HSCT and tested univariately using Gray test. For GF, our primary outcome measure, we performed multivariate analysis using Fine-Gray competing risk regression, using stepwise selection, and including all variables that increase model strength, assessed using the Bayesian Information Criterion (BIC). Multinomial logistic regression was used to investigate the incidence of mixed chimerism at 1 year, accounting for death and GF. To compare group medians of immune cell populations, the Wilcoxon signed rank test and Tukey boxplots were used. *P* values were considered of statistical significance at the level of <.05. Our main exposure parameter of interest was the estimated alemtuzumab concentration at day 0 (C_{tx}), because it is unaffected by graft dose and variables occurring after transplantation, which may be related to the outcomes of interest, thus avoiding potential biases. This exposure parameter is less influenced by the date of first alemtuzumab dose than the AUC until HSCT and it allows for easy replication studies because it can be assessed in a single sample. This choice was made before comparing different exposure parameters. We categorized exposure by using quantiles and medians and used the most informative exposure by assessing informativeness of categorization using BIC on a composite outcome Cox model predicting mortality and GF. We also assessed an optimal categorization by identifying 2 cut points that minimized the sum of squared deviance residuals using the same Cox model but refrained from using this categorization on other outcomes, because it was highly dependent on the observed outcome, invalidating model assumptions and only determined it to have a "best guess" optimal dosing window. This method differs from previously published decision-tree algorithms,[15] which only optimize a single split at a time, thereby possibly leading to suboptimal ranges. In contrast to a decision tree, this method is not a hierarchical model but optimizes 2 splits to achieve 3 categories. As such, minimum node size, covariates, and pruning are not applicable; the problem space is much smaller; and the potential of overfitting much lower.

Results

PK model development and validation

Alemtuzumab was measured in 698 samples from 53 children, 18 of which were recruited prospectively. Data overlap with a previous retrospective study[21] is limited to 32% (17 of 53) of patients. Patient and transplant characteristics are summarized in Table 1.

Table 1. Patient and transplant characteristics, ungrouped and by alemtuzumab exposure

Characteristic	Ungrouped	By median exposure		
	N = 53*	Low exposure, n = 27*	High exposure, n = 26*	*P* value†
Diagnosis				.012
ADA2 deficiency	1 (1.9%)	0 (0%)	1 (3.8%)	
APDS type 1	1 (1.9%)	1 (3.7%)	0 (0%)	
CGD	8 (15%)	5 (19%)	3 (12%)	
CID	1 (1.9%)	0 (0%)	1 (3.8%)	
Congenital severe thrombopenia	1 (1.9%)	1 (3.7%)	0 (0%)	
CTLA-4 deficiency	1 (1.9%)	0 (0%)	1 (3.8%)	
DOCK8 mutation	1 (1.9%)	1 (3.7%)	0 (0%)	
HLH	7 (13%)	4 (15%)	3 (12%)	
Hyper-IgE syndrome	1 (1.9%)	1 (3.7%)	0 (0%)	
IFNgR1 deficiency	7 (13%)	5 (19%)	2 (7.7%)	
IL10RB deficiency	2 (3.8%)	2 (7.4%)	0 (0%)	
IPEX	2 (3.8%)	2 (7.4%)	0 (0%)	
MKL1 mutation	1 (1.9%)	1 (3.7%)	0 (0%)	
SAA	6 (11%)	0 (0%)	6 (23%)	
SCID	10 (19%)	2 (7.4%)	8 (31%)	
Shwachman-Diamond syndrome	1 (1.9%)	1 (3.7%)	0 (0%)	
STIM1	1 (1.9%)	1 (3.7%)	0 (0%)	
WAS	1 (1.9%)	0 (0%)	1 (3.8%)	
Diagnosis category				.14
Hematological	8 (15%)	2 (7.4%)	6 (23%)	
IEI	45 (85%)	25 (93%)	20 (77%)	
Sex				.5
Female	20 (38%)	9 (33%)	11 (42%)	
Male	33 (62%)	18 (67%)	15 (58%)	
Age at HSCT, y	4.4 (0.8-8.7)	4.0 (0.7-8.6)	4.9 (1.4-9.8)	.5
Alemtuzumab treatment				
Cumulative dose mg/kg,	0.60 (0.60-1.00)	0.60 (0.55-0.60)	0.90 (0.60-1.00)	.01
Start day before HSCT	−11.0 (−14.0 to −8.0)	−12.0 (−14.0 to −10.0)	−8.0 (−11.8 to −7.2)	.003
No. of doses	4 (2-7)	3 (3-4)	4 (3-5)	.069
Conditioning				.021
Busulfan, fludarabine	12 (23%)	5 (19%)	7 (27%)	
Fludarabine, cyclophosphamide	6 (11%)	0 (0%)	6 (23%)	
Fludarabine, treosulfan	18 (34%)	10 (37%)	8 (31%)	
Fludarabine, treosulfan, thiotepa	17 (32%)	12 (44%)	5 (19%)	
Intensity of conditioning				.2
Myeloablative	21 (40%)	13 (48%)	8 (31%)	
Reduced	32 (60%)	14 (52%)	18 (69%)	
GVHD prophylaxis				.3
Cyclosporine	7 (13%)	2 (7%)	5 (19%)	
Cyclosporine, MMF	15 (28%)	7 (26%)	8 (31%)	
Cyclosporine, MTX	23 (43%)	12 (44%)	11 (42%)	

Based on the median alemtuzumab concentration at day of HSCT (0.77 μg/mL), patients were stratified into the high-exposure (>0.77 μg/mL) or low-exposure groups (≤0.77 μg/mL).

ADA2, adenosine deaminase; APDS, activated PI3 kinase delta syndrome; BM, bone marrow; CB, cord blood; CGD, chronic granulomatous disease; CTLA4, cytotoxic T-lymphocyte associated protein 4; CID, combined immunodeficiency; DOCK8, dedicator of cytokinesis 8; HAPLO, haploidentical; HLH, hemophagocytic lymphohistiocytosis; IgG, immunoglobulin G; IEI, inborn errors of immunity; IFNgR1, interferon γ receptor 1; IL10RB, interleukin 10 receptor subunit β; IPEX, immunodysregulation polyendocrinopathy enteropathy X-linked syndrome; MMD, mismatched donors; MMF, mycophenolate mofetil; MRD, matched related donors; MTX, methotrexate; MUD, matched unrelated donors; PBSC, peripheral blood stem cells; SAA, severe aplastic anemia; SCID, severe combined immunodeficiency; STIM1, stromal interaction molecule; WAS, Wiskott-Aldrich syndrome.

*n (%); median (interquartile range).

†Fisher exact test; Pearson χ^2 test; Wilcoxon rank-sum test.

Table 1 (continued)

Characteristic	Ungrouped	By median exposure		
	N = 53*	Low exposure, n = 27*	High exposure, n = 26*	*P* value†
MTX, MMF	1 (2%)	1 (4%)	0 (0%)	
Cyclosporine, MMF, post-cyclophosphamide	5 (9%)	5 (19%)	0 (0%)	
No	2 (4%)	0 (0%)	2 (8%)	
Graft source				.7
BM	39 (74%)	21 (78%)	18 (69%)	
CB	6 (11%)	2 (7.4%)	4 (15%)	
PBSC	8 (15%)	4 (15%)	4 (15%)	
Graft manipulation				.7
CD34 selection	5 (10%)	2 (7%)	3 (12%)	
No	48 (91%)	25 (93%)	23 (88%)	
Donor type				.025
MRD	12 (23%)	10 (37%)	2 (8%)	
HAPLO	2 (3.8%)	0 (0%)	2 (8%)	
MMD	17 (32%)	6 (22%)	11 (42%)	
MUD	22 (42%)	11 (41%)	11 (42%)	
Follow-up post-HSCT, y	3.3 (2.5-8.0)	2.8 (2.0-3.7)	6.8 (2.8-10.6)	.005

Based on the median alemtuzumab concentration at day of HSCT (0.77 μg/mL), patients were stratified into the high-exposure (>0.77 μg/mL) or low-exposure groups (≤0.77 μg/mL).
ADA2, adenosine deaminase; APDS, activated PI3 kinase delta syndrome; BM, bone marrow; CB, cord blood; CGD, chronic granulomatous disease; CTLA4, cytotoxic T-lymphocyte associated protein 4; CID, combined immunodeficiency; DOCK8, dedicator of cytokinesis 8; HAPLO, haploidentical; HLH, hemophagocytic lymphohistiocytosis; IgG, immunoglobulin G; IEI, inborn errors of immunity; IFNgR1, interferon γ receptor 1; IL10RB, interleukin 10 receptor subunit β; IPEX, immunodysregulation polyendocrinopathy enteropathy X-linked syndrome; MMD, mismatched donors; MMF, mycophenolate mofetil; MRD, matched related donors; MTX, methotrexate; MUD, matched unrelated donors; PBSC, peripheral blood stem cells; SAA, severe aplastic anemia; SCID, severe combined immunodeficiency; STIM1, stromal interaction molecule; WAS, Wiskott-Aldrich syndrome.
*n (%); median (interquartile range).
†Fisher exact test; Pearson χ^2 test; Wilcoxon rank-sum test.

Sampling time points ranged from 15 to 30 minutes after completing the infusion of the first alemtuzumab dose, up to 104 days thereafter, thereby covering the PK curve of the entire patient group. The number of samples per patient ranged from 7 to 28, with a median of 13 samples. A 2-compartment disposition model with parallel first order (linear) and Michaelis–Menten (nonlinear) elimination kinetics best described the PKs of alemtuzumab in this patient group (electronic supplemental Material; supplemental Figure 2). The main steps of the model building process are summarized in the electronic supplemental Material; supplemental Table 2. Before covariate analysis, the observed interindividual variability (IIV) was 93.5% (relative standard error [RSE], 0%) for drug clearance and 105.8% (RSE, 10%) for the volume of distribution. Analysis of potential covariates (electronic supplemental Material; supplemental Table 1) identified total bodyweight (allometrically scaled to account for body size–related differences) as a significant predictor of alemtuzumab CL (electronic supplemental Material; supplemental Figure 3) and Vd. Lymphocyte count at baseline was identified as a significant predictor of alemtuzumab linear and nonlinear CL but not of Vd (electronic supplemental Material; supplemental Figure 4).

After the inclusion of bodyweight and baseline lymphocyte count in the PK model, model–estimated average drug CL was 0.214 L per day (RSE, 11%) with a significantly reduced IIV of 74.4% (RSE, 14%). Average Vd was estimated to be 0.985 L (RSE, 14%) with a significantly reduced IIV of 41.5% (RSE, 18%). Residual variability was characterized by a combined error model with an additive error of 0.0231 μg/mL and a proportional error of 27.9% (expressed as the coefficient of variation). All final model–estimated PK metrics after bootstrap simulation (1000 runs) are reported in Table 2. The final model analysis revealed no structural bias or major deviations (electronic supplemental Material; supplemental Figure 5) and a good agreement between observed and predicted alemtuzumab concentrations, with most of the observations falling within the 90% prediction interval (electronic supplemental Material; supplemental Figure 8A-B). Additional evidence for the predictive strength of this model for its current purpose was provided by the strong correlation between measured alemtuzumab concentrations at day of HSCT (±1 day) and corresponding model-estimated concentrations (electronic supplemental Material; supplemental Figure 8C). The observed and individual model predicted concentration-time curves of this cohort are displayed in Figure 1B. Individual plots per patient are shown in the electronic supplemental Material (supplemental File 2).

Exposure-response analysis

To analyze the correlation between alemtuzumab exposure and clinical outcome of interest, the previously described model-derived exposure metrics were used (electronic supplemental Material; supplemental Table 2).

Although the day on which alemtuzumab reaches its lympholytic level of <0.1 μg/mL (36 days after HSCT, 95% confidence interval [CI], 28-41) better expresses the entire exposure period, we reasoned that alemtuzumab levels after HSCT might be influenced by variables occurring after transplantation, which may be related to the outcomes of interest. For exposure-response analysis, we

Table 2. Population PK parameters of the final model and 1000 bootstrap runs

	Final population PK model			1000 bootstrap run results	
	Mean value	RSE (%)	Shrinkage (%)	Median value	95% CI
$CLi = CLpop \times \left(\frac{WT}{WT_{med}}\right)^{(WT)^{0.75}} \times$ **(1 + (LY/LYmed × 0.8)** ***WTmed = 18 kg, LYmed = 2.2410 × 10⁹/L***					
CLpop (L per day)	0.214	11		0.210	0.11-0.32
Exponent WTmed on CLpop (fixed)	0.75			0.75	
Linear function LYmed on CLpop	0.8	29		0.88	0.09-2.85
$Vdi = Vdpop \times \left(\frac{WT}{WT_{med}}\right)^{(WT)^{1}}$ ***WTmed = 18 kg***					
Vdpop (L)	0.985	14		0.994	0.717-1.32
Exponent WTmed on Vd (fixed)	1			0.75	
K21/d	2.63	16		2.52	1.33-3.30
Tmax (mg per day)	22.3	29		22.17	8.49-38.02
Tm (μg/mL)	2.23	42		2.15	1.25-5.74
Vmax (mg per day)	0.0438	23		0.0485	0.026-0.255
Km (μg/mL)	0.633	19		0.605	0.229-8.142
IIV					
CL (CV%)	74.4	14	0	73.1	53.5-95.7
Vd (CV%)	41.5	18	21	42.2	25.6-58.2
Tm (CV%)	114.5	13	7	111.9	86.6-144.4
Km (CV%)	195.4	29	58	162.3	77.0-586.0
Random residual variability					
Proportional (CV%)	27.9	7	9	27.6	24.0-32.4
Additive (μg/mL)	0.0231	23	9	0.0225	0.0006-0.034

K21, transfer rate constants connecting compartments; Tmax, maximum transport rate of distribution toward peripheral compartment; Tm, Michaelis–Menten constant saturable distribution toward peripheral compartment; Vmax, maximum elimination rate; Km, concentration at which the elimination pathway is half saturated; CV%, percentage coefficient of variation.

selected the median model–estimated alemtuzumab concentration at day of HSCT (0.77 μg/mL; interquartile range, 0.33-1.82; Figure 1A), which correlated strongly with the day on which the alemtuzumab concentration reached its lympholytic level after HSCT (electronic supplemental Material; supplemental Figure 7A-B), and has the additional advantage that it may have practical applicability in the clinical context.

Model–estimated alemtuzumab concentration at day of HSCT was categorized into quartiles (Q1, <0.33 μg/mL; Q2, 0.33-0.77 μg/mL; Q3, 0.771-1.82 μg/mL; and Q4, >1.82 μg/mL) and into 2 groups defined by the median value as the "low-exposure" (≤0.77 μg/mL) and "high-exposure" (>0.77 μg/mL) groups. Exposure-response analysis was assessed based on both exposure groups defined by quartiles or by the median exposure value and results were compared. Because the use of quartiles did not provide any information gain, this manuscript only provides analysis results based on the median model–estimated alemtuzumab concentration at day of HSCT (exposure C_{tx}). Table 1 provides patient characteristics also per the exposure group.

The results of the quartiles-based exposure-response analysis of T- and NK cell recovery are reported in the electronic supplemental Material (supplemental Figure 11).

Immune reconstitution

After transplantation, patients reached $CD4^+$ and $CD8^+$ T-cell recovery at a median time of 48 days (95% CI, 33-76) and 78 days (95% CI, 39-113), respectively. In exposure-response analysis, a significant correlation between alemtuzumab exposure C_{tx} and T-cell recovery was observed. In patients with high alemtuzumab exposure, the median time to $CD4^+$ and $CD8^+$ T-cell recovery was strongly delayed in comparison with the low-exposure group (Figure 2A-B; electronic supplemental Material; supplemental Figures 12-14). Likewise, the absolute count of naïve and memory/effector $CD4^+$ and $CD8^+$ subpopulations was significantly lower in the high-exposure group at 1 and 3 (except for memory/effector $CD8^+$ cells) months after transplantation but not later (supplemental Figures 13 and 14).

NK cells recovered in 88.7% of patients (47 of 53) at a median time of 33 days (95% CI, 28-35) after transplantation and delayed NK cell recovery was associated with higher alemtuzumab exposure C_{tx} ($P = .019$, Figure 2C).

No significant correlation was observed between alemtuzumab exposure C_{tx} and time of neutrophil, monocyte, and $CD19^+$ B-cell recovery (electronic supplemental Material; supplemental Figures 15 and 16).

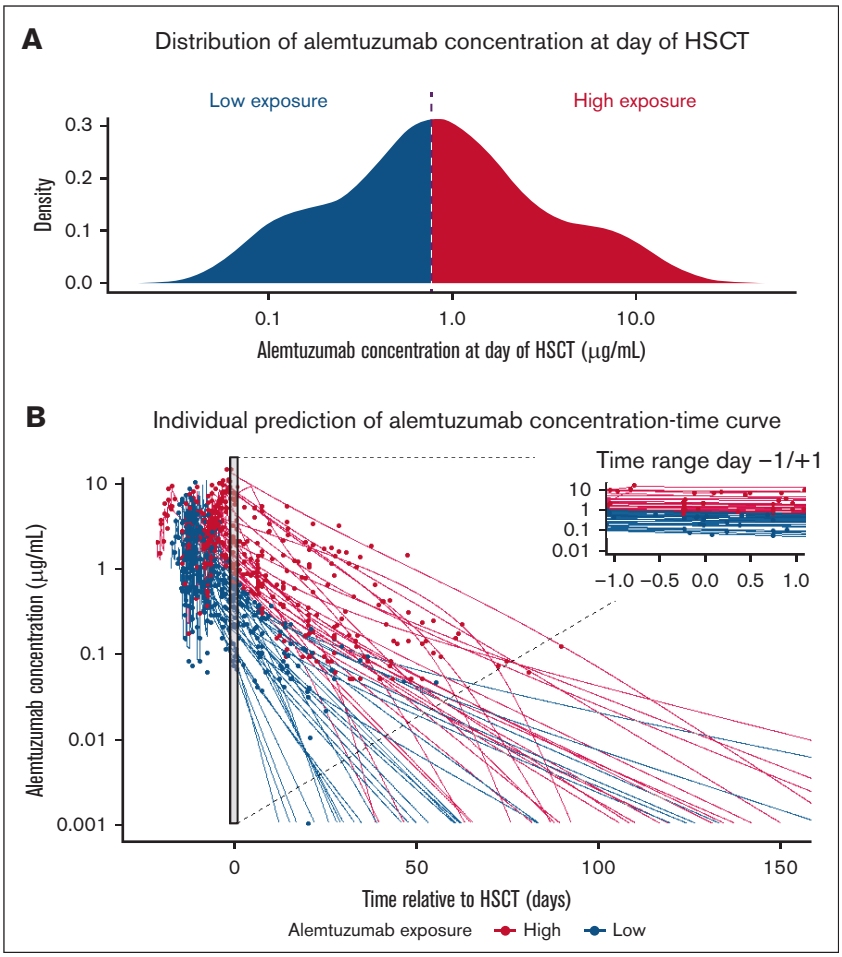

Figure 1. Alemtuzumab PKs by exposure group at day of HSCT. (A) Distribution of estimated alemtuzumab concentration at day of HSCT. Based on the median value (0.77 µg/mL, blue vertical dotted line), patients were divided into the high-exposure (>0.77 µg/mL, red area) or low-exposure (≤0.77 µg/mL, blue area) groups. (B) Alemtuzumab observed concentrations (dots) and model–estimated individual PK predictions (solid lines). Patients of the high-exposure group are represented in red, and patients of the low-exposure group are represented in blue.

To address the influence of $CD34^+$-selected grafts (n = 5) or postcyclophosphamide-based T-cell depletion (PTCy, n = 5) on immune reconstitution, we performed a sensitivity analysis on 43 patients who neither receive a $CD34^+$-selected graft nor PTCy. In this cohort, the median concentration at day of HSCT was slightly higher than in the original cohort (0.87 vs 0.77 µg/mL) and ahigh alemtuzumab exposure (concentration at day of HSCT of >0.87 µg/mL) correlated significantly with a delayed recovery of $CD4^+$ ($P < .0001$) and $CD8^+$ ($P = .00078$) T cells (electronic supplemental Material; supplemental File3; supplemental Figure 2A-B). In addition, we observed a trend toward delayed NK cell recovery at a high alemtuzumab exposure, but in this cohort the correlation did not reach statistical significance ($P = .064$; electronic supplemental Material; supplemental File 3; supplemental Figure 2C).

GF, mortality, and event free survival (EFS)

Primary GF occurred in 2 patients (3.8%), who first received autologous stem cells to recover from hematological aplasia and then successfully received retransplantation after a different conditioning regimen with the same or an alternative donor. In total, 5 patients (9.4%) experienced a secondary GF leading to a second allogeneic HSCT, which was mostly performed (3 of 5) with a second donor. In competing risk analysis accounting for death, the cumulative incidence of GF was 13.6% and significantly correlated with alemtuzumab exposure C_{tx} ($P = .043$, Figure 3A-B). For the incidence of GF, our primary outcome measure, we performed multivariate analysis using Fine-Gray competing risk regression based on forward stepwise selection and including all variables that may increase the strength of the model, assessed using the BIC. Our findings revealed that the best model was the model based on the alemtuzumab concentration at day of HSCT and without any additional covariates. To demonstrate that no other model performed better than the selected model, we also performed an analysis of variance, which showed no improvement with a very similar logarithmic likelihood of −24.4 for the univariate and −24.1 for the bivariate model and a corresponding P value of .39. As we believe our study is not sufficiently powered to properly assess the effect of multiple covariates simultaneously in a multivariate analysis, and did not include a multivariate analysis in the design of this study, the analysis results are only reported in the electronic supplemental Material (supplemental Tables 3 and 4).

Of the 9 deaths (17%), 4 were attributed to respiratory failure, 3 to disseminated aspergillosis, 1 to multiorgan failure, and 1 to progressive preexistent neurodegeneration. The cumulative incidence of mortality accounting for second HSCT as competing risk factor was 11.4%. In the univariate analysis, there was no evidence for a significant correlation between alemtuzumab exposure and risk of

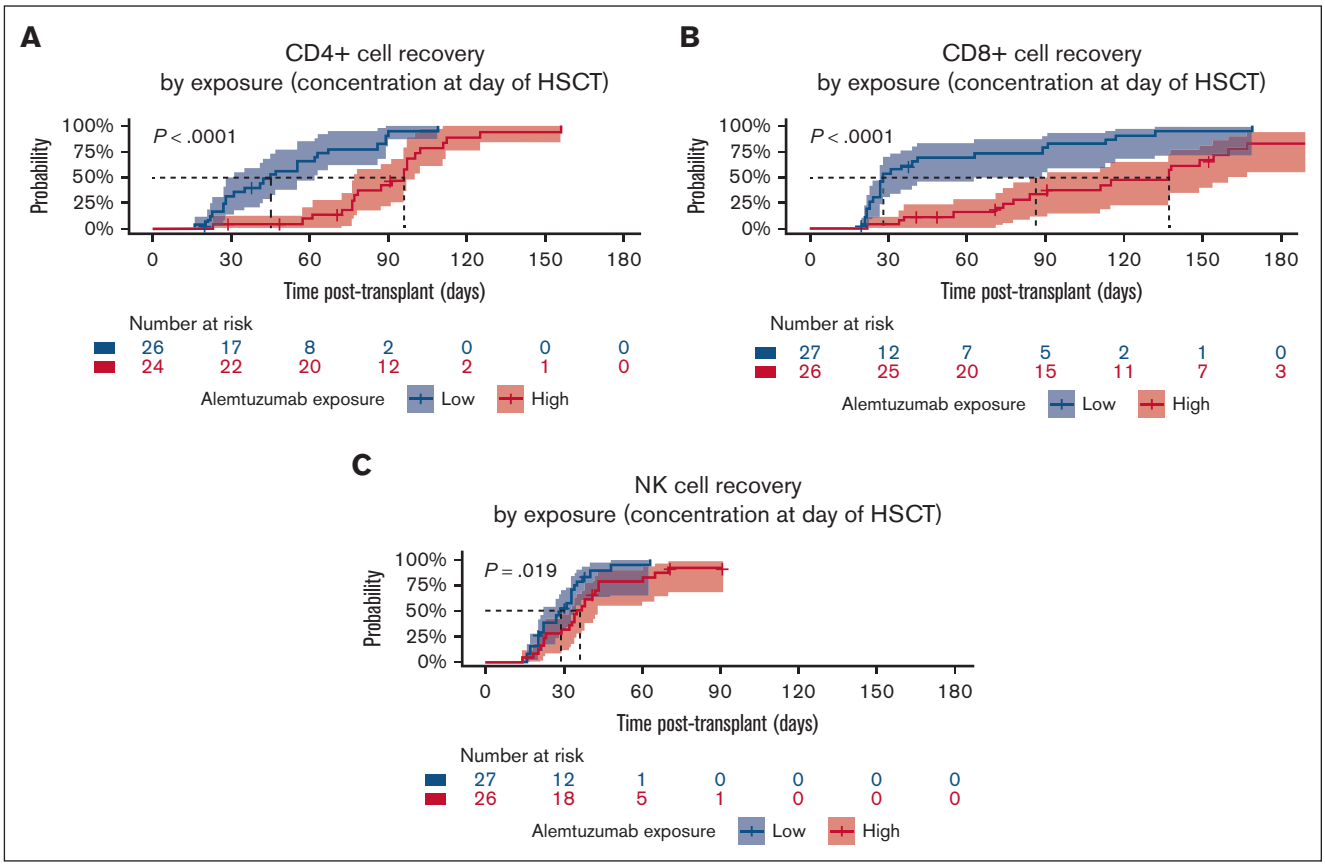

Figure 2. T-cell and NK cell recovery by alemtuzumab exposure at day of HSCT. Kaplan-Meier estimates for patients stratified based on the median estimated alemtuzumab concentration at day of HSCT (0.77 μg/mL) into high-exposure (>0.77 μg/mL, represented in red) or low-exposure (≤0.77 μg/mL, represented in blue) groups. Dotted black lines represent the median recovery time for each exposure group. (A) $CD4^+$ T-cell recovery (>0.05 × 10^9/L), median time: 45 days (95% CI, 28-62, low exposure) vs 96 days (95% CI, 77-100 days, high exposure). (B) $CD8^+$ T-cell recovery (>0.05 × 10^9/L), median time: 28 days (95% CI, 27-89, low exposure) vs 137 days (95% CI, 91-167, high exposure). (C) NK cell recovery (>0.05 × 10^9/L), median time: 29 days (95% CI, 22-35 days, low exposure) vs 36 days (95% CI, 32-43, high exposure).

mortality (Figure 3C-D), which, however, was significantly associated with the type of donor ($P = .013$).

We attempted to identify the optimal alemtuzumab exposure C_{tx} range by splitting the data in 3 categories, determining split points by minimizing squared deviance residuals for EFS, defined by GF and death as events. The split points were as follows: low-exposure C_{tx} (concentration <0.18 μg/mL), intermediate-exposure C_{tx} (concentration between 0.18 and 0.58 μg/mL), and high-exposure C_{tx} (concentration >0.58 μg/mL). Although no events occurred in the intermediate-exposure group (n = 13), the 1-year EFS in the low-exposure and high-exposure groups was 56% (95% CI, 31%-100%) and 71% (95% CI, 57%-89%), respectively (electronic supplemental Material; supplemental Figure 10). Because groups were defined based on outcomes, corresponding *P* values were not determined.

Acute and chronic GVHD

Two patients developed grade 1 (3.8%) and 6 children experienced grade 2 (11.3%) aGVHD. There were no patients with aGVHD grade 3 or 4 in this cohort. We considered aGVHD of at least grade 2 to be clinically relevant. The overall incidence of aGVHD grade 2, accounting for aGVHD grade 1, death, and second HSCT as competing risk factors, was 11.5% and no significant correlation with alemtuzumab exposure C_{tx} was observed in exposure-response analysis (Figure 3E-F). The multivariate analysis of aGVHD, the further main indication for alemtuzumab treatment before HSCT, was performed by using Fine-Gray competing risk regression based on forward stepwise selection and including all variables that may increase model strength. Moreover, we applied the BIC for model selection, which revealed that the best model was the model based on the alemtuzumab concentration at day of HSCT and without any additional covariates. Our findings are reported in the electronic supplemental Material (supplemental Tables 3 and 4).

Accounting for the low incidence of aGVHD, a sensitivity analysis addressing aGVHD grade 1 to 2 was performed and provided no major changes (data not shown). One patient each of the low- (1.9%) and high-exposure (1.9%) groups developed chronic GVHD of limited grade.

Chimerism

To investigate chimerism, we tabulated clinical outcome (GF and survival) at 1 year after HSCT, at which we had no loss to follow-up. Although 26 patients were alive with full donor chimerism, 14 patients had mixed donor chimerism: 6 in the low-exposure group

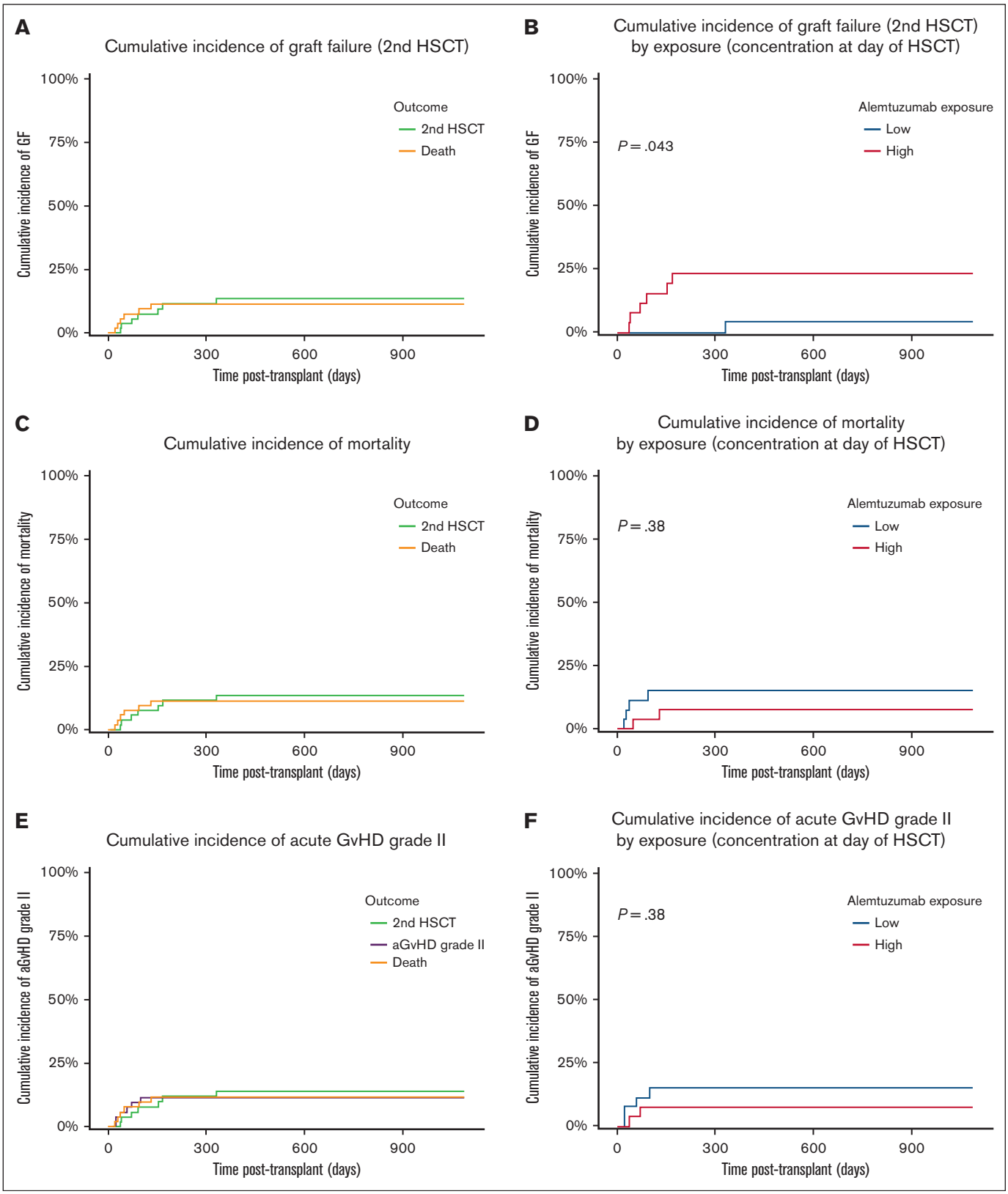

Figure 3. Exposure-response competing risk analysis of GF, mortality, and aGVHD. Based on the median concentration at the day of transplant (0.77 μg/mL), patients were stratified into the high-exposure group (>0.77 μg/mL, represented in red) or into the low-exposure group (≤0.77 μg/mL, represented in blue). (A) Overall cumulative incidence of GF (second HSCT, green line) accounting for death as competing risk (yellow line). (B) Cumulative incidence of GF (second HSCT) in correlation with alemtuzumab

and 8 in the high-exposure group at day of HSCT. Clinical outcome at 1 year was not significantly different between the exposure groups (Fisher exact $P = .34$; electronic supplemental Material; supplemental Table 5).

Using multinomial logistic regression, taking being alive with full donor chimerism as the reference category, we further evaluated the outcome-specific influence of alemtuzumab exposure C_{tx} on the incidence of being alive with mixed chimerism, death, or GF at 1 year after HSCT and observed no statistically significant correlation ($P = .26$ and logistic odds = 0.76 for being alive with mixed chimerism; $P = .56$ and logistic odds = 0.47 for death; $P = .12$ and logistic odds = 1.86 for GF).

Viral reactivations

Of 31 patients (58.5%) at risk based on pre-HSCT serostatus, 14 (45.2%) experienced a CMV reactivation. Seven (22.6%) children were treated with antiviral medication for at least 2 weeks, thus indicating poor T-cell recovery, which is essential for CMV control. Analysis accounting for death and second HSCT as competing risks revealed a cumulative incidence of CMV reactivation of 19.0% (electronic supplemental Material; supplemental Figure 17A). In univariate analysis, alemtuzumab exposure C_{tx} was neither associated with the incidence of CMV reactivations nor with a duration of CMV treatment of at least 2 weeks (electronic supplemental Material; supplemental Figure 17B-D). Age ($P = .03$) and donor-type ($P = .004$) were identified as significant predictors of the incidence of CMV reactivations.

Of the 42 patients at risk, 10 (23.8%) developed an Epstein-Barr virus reactivation, 26.4% (14 of 53) of patients were diagnosed with an adenovirus infection, and neither of them was correlated with alemtuzumab exposure C_{tx} (electronic supplemental Material; supplemental Figure 18).

Autoimmunity

In 13.2% of patients who were included (7 of 53), the clinical course after transplantation was complicated by the onset of hematological (n = 3; 5.7%) or nonhematological (n = 4; 7.5%) autoimmunity. Of 7 patients, 6 developed autoimmunity within 1 year of follow-up in the presence of full donor chimerism ($P < .001$) but alemtuzumab exposure C_{tx} was not identified as a significant predictor of autoimmunity (electronic supplemental Material; supplemental Figure 19).

Discussion

To elucidate the PK properties of intravenous alemtuzumab in children undergoing HSCT for nonmalignant diseases, and their impact on the outcome after transplantation, we conducted a combined prospective/retrospective observational trial including 53 patients and performed, to our knowledge, the first model–estimated exposure-response analysis in this patient population. Our findings revealed that high alemtuzumab exposure expressed by the concentration at the day of HSCT (exposure C_{tx}) correlated with delayed T-cell recovery and increased risk of GF.

A large amount of concentration-time data collected during the entire period of alemtuzumab distribution and elimination allowed the development of a 2-compartment population PK model with parallel linear and nonlinear clearance, which accounted for both nonspecific and target-mediated drug elimination and provided sufficient predictive performance. Allometrically scaled bodyweight and lymphocyte count at baseline were identified as relevant predictors of alemtuzumab clearance and need to be considered for future dosing optimization. However, substantial unexplained IIV persisted despite model inclusion of both predictors of clearance, thus further supporting the complexity of alemtuzumab PK in this patient population. This novel model–estimated prediction may be considered as the best possible in this patient population. Model-informed precision dosing with individualized alemtuzumab dosing based on the final population PKs model in combination with measured alemtuzumab concentrations shortly after the first administration may be the best way forward to optimize alemtuzumab treatment in this patient population. Because the start of alemtuzumab treatment and the cumulative alemtuzumab dose differed significantly between the low- and high-exposure groups at day of HSCT in our cohort, we infer that both initial dose individualization and subsequent dose adjustment (therapeutic drug monitoring by Bayesian forecasting) based on a population PKs model also need to be taken into account as important determinants of alemtuzumab PKs for optimal individualized dosing. Although the administration route was shown to influence alemtuzumab biodistribution and clearance,[34] the median estimated alemtuzumab concentration observed at day of HSCT in our cohort was comparable with the results reported in children treated subcutaneously with similar dosing regimens and timing of administration.[15,35] Further insight in the residual alemtuzumab PK variability may be revealed by pharmacogenomic analysis. Because the strength of antibody-dependent cell-mediated cytotoxicity response, the key mechanism of alemtuzumab action,[7-12] was shown to be influenced by immunoglobulin Fcγ receptor polymorphism,[36,37] pharmacogenomic analysis addressing these particular polymorphic variants may be of interest for future studies.

Alemtuzumab population PK analysis has previously been performed by our group and led to the development of a population PKs model in an historic pediatric HSCT cohort of malignant and nonmalignant diseases.[21] Although the previous 2-compartment population PK model was based on parallel saturable and linear drug elimination and only identified bodyweight as relevant PK predictor using a stepwise power function, this novel model also identified the lymphocyte count at baseline as significant predictor of clearance possibly because of different baseline lymphocyte count characteristics of this addressed nonmalignant pediatric population. The previous population PK model has also been evaluated on this study population and model-estimated values of linear clearance were comparable with our findings (0.25 vs 0.214 L per day). In contrast, Vd, maximal elimination rate, and concentration at which the elimination pathway is half saturated were slightly different. Evaluation of models' GOF (electronic supplemental Material; supplemental Figure 6) revealed that this

Figure 3 (continued) exposure. (C) Overall cumulative incidence of mortality (yellow line) accounting for GF (second HSCT, green line) as competing risk. (D) Cumulative incidence of mortality in correlation with alemtuzumab exposure. (E) Overall cumulative incidence of aGVHD (purple line) accounting for GF (second HSCT, green line) and death (yellow line) as competing risks. (F) Cumulative incidence of aGVHD in correlation with alemtuzumab exposure.

novel population PK model better describes the PK characteristics of the addressed nonmalignant pediatric population, thus providing less residual IIV and allowing higher predictive power for the first model–based exposure-response analysis in this cohort.

In this study, the median estimated alemtuzumab concentration at the day of transplantation was markedly above the estimated drug lympholytic level (0.1 μg/mL) and fell below this level at a median of 36 days after HSCT, thus pointing to the potential impact of alemtuzumab on immune-mediated events during the early posttransplant course. In line with prior reports,[30] a high alemtuzumab exposure, defined by exposure C_{tx} of at least 0.77 μg/mL, strongly correlated with a delayed recovery of $CD4^+$ and $CD8^+$ T cells until 3 months after transplantation. Similarly, both naïve and memory/effector $CD4^+$ and $CD8^+$ T cells showed a delayed appearance over the first 3 months after transplantation. Despite a high CD52 expression, B-cell reconstitution did not correlate significantly with exposure C_{tx}, but this may be a consequence of their generally late reconstitution in comparison with T cells.

Considering that the use of $CD34^+$-selected grafts or PTCy may influence the immune reconstitution, a sensitivity analysis on patients who neither receive a $CD34^+$-selected graft nor PTCy was performed. In this subgroup analysis, a significant delayed recovery of $CD4^+$ and $CD8^+$ T cells but not of NK cells has been confirmed. However, taking the limited number of recipients of $CD34^+$-selected grafts (n = 5) or PTCy (n = 5) into account, conclusions on their effective influence on alemtuzumab PKs and on NK cell recovery need to be drawn cautiously.

Early T-cell recovery may have a major impact on the quality of life of children who have received transplants because of its impact on graft function, duration of antimicrobial prophylaxis, need for immunoglobulin supplementation, and lifestyle recommendations. Strategies to accelerate early T-cell recovery without concomitant disadvantageous alloreactivity may strongly contribute to achieve a favorable outcome.

In addition, high alemtuzumab exposure C_{tx} correlated with a higher incidence of GF. As to the best of our knowledge, no optimal theoretical exposure range has previously been defined for intravenous alemtuzumab treatment, we attempted to identify exposure C_{tx} leading to the best possible EFS at 1 year. Because neither death nor second HSCT occurred in 13 children with alemtuzumab concentrations between 0.18 and 0.58 μg/mL, this concentration range may represent the optimal alemtuzumab exposure target on the day of HSCT in this category of patients.

Our results reflect previously reported concentrations between 0.2 and 0.4 μg/mL at the day of HSCT, which have been associated with significantly lower incidences of aGVHD and mixed chimerism, whereas concentrations of >0.6 μg/mL on the day of transplantation were associated with delayed immune reconstitution in children and young adults after subcutaneous treatment.[15] Aiming at identifying optimal subcutaneous alemtuzumab dosing, a 1-compartment population PK model with linear elimination and including bodyweight (allometrically scaled) as relevant covariate on alemtuzumab clearance was recently developed, which suggested the use of model-informed precision dosing based on bodyweight or body surface area to achieve an optimal exposure C_{tx} of 0.15 to 0.6 μg/mL at the day of HSCT.[22] As stated by Dong and et al,[22] the different administration route and treatment protocol with diverse dosing, a smaller sample size, and more sparse PK sampling protocol in their data set may explain the different PK parameter estimates and the significantly reduced model performance (GOF) when tested on this study data set (electronic supplemental Material; supplemental Figure 7). Our model prediction based on data after intravenous alemtuzumab administration is comparable with the reported population PK model fit after subcutaneous administration. However, our analysis of optimal exposure C_{tx} was merely exploratory and may be influenced by a variable exposure before HSCT resulting from predictors such as alemtuzumab dosing and timing. These findings need to be confirmed in larger prospective trials addressing model-informed precision dosing or in a meta-analysis combining all available raw data. In addition, it would be very interesting to combine all available data of previously published models of alemtuzumab PK/pharmacodynamics in malignant and nonmalignant diseases to investigate whether there are any significant differences between malignant and nonmalignant populations.

In contrast with the mentioned previous report,[15] which highlighted an association with the incidence of aGVHD in the low-exposure group, we did not observe a significant correlation between alemtuzumab exposure C_{tx} and the incidence of aGVHD and mixed chimerism. Although the events (ie, GF and deaths due to severe infections) occurring in the low-exposure group in our study may seem less intuitive, they may be related to the differences in conditioning regimens and patient populations with variable underlying diseases. Moreover, the differing chimerism results may be explained by the different methodology used to analyze this specific outcome. We decided to investigate chimerism at 1 year using multinomial logistic regression to account for competing events and patients switching from mixed to full donor chimerism over time. Future studies in larger cohorts will provide further insights into these possible relationships.

Because available literature reported on outcome-specific associations with different parameters of antithymocyte globulin exposure,[38] we performed multivariate analysis addressing the association between several parameters of alemtuzumab exposure and the incidence of GF as well as aGVHD grade 2 in this patient population and did not find any major changes (electronic supplemental Material; supplemental Figure 20). Alemtuzumab model–estimated AUC pre-HSCT and cumulative AUC provided the strongest trend of all exposure parameters toward reduced risk of aGVHD grade 2 with high alemtuzumab exposure (electronic supplemental Material; supplemental Table 4). However, because model-estimated concentration at day of HSCT is less influenced by the date of first alemtuzumab dose than the AUC before HSCT, we selected this exposure parameter also for the analysis of aGVHD. In conclusion, our findings support a strong correlation between alemtuzumab exposure C_{tx} and T-cell reconstitution as well as incidence of GF and, therefore, the need for individualized treatment approaches. In this patient population, our results suggest an optimal concentration range of 0.18 to 0.58 μg/mL at the day of HSCT, which is similar to the results reported for subcutaneous administration but different in the nature of adverse events,[15,35] but this range needs to be confirmed and may be different in other clinical settings. This novel population PK model will allow model-informed precision dosing using limited sampling

protocols combined with Bayesian estimation of alemtuzumab concentrations, aiming at the achievement of early T-cell reconstitution and prevention of GF in future prospective studies.

Acknowledgments

The authors thank the medical staff of both study centers for collecting patient samples, and all patients and their families for participating in this study. The authors gratefully acknowledge the Flow cytometry Core Facility of Leiden University Medical Center, coordinated by Koen Schepers, and Marjolijn Hameetman for facilitating the use of flow cytometers (https://www.lumc.nl/research/facilities/fcf).

This work was supported by Willem-Alexander Children's Hospital, Leiden University Medical Center, Leiden, The Netherlands, grants of the Children's Research Centre of the University Children's Hospital Zurich (FZK-2018-INV-031), and grants from private foundations Aldo and Cele Daccò Foundation, EMDO Foundation (999), Wolfermann-Nägeli Foundation, Zurich, Switzerland (F.R.A.-G.).

The funders had no role in study design data collection and analysis, decision to publish, or preparation of the manuscript.

Authorship

Contribution: F.R.A.-G. contributed to the research design, performed research, analyzed data, and wrote the manuscript; D.J.A.R.M. and E.G.J.v.A. analyzed data and wrote the manuscript; T.G. and A.C.L. contributed to the research design, performed research, and wrote the manuscript; and R.G.M.B., M.W.S., C.M.J.-v.d.Z., M.J.D.v.T., and A.M.J.-H. performed research and revised the manuscript.

Conflict-of-interest disclosure: The authors declare no competing financial interests.

ORCID profiles: F.R.A.-G., 0000-0002-0797-8146; M.W.S., 0000-0003-4391-6003; E.G.J.v.A., 0000-0001-6256-7457; C.-M.J.-v.d.Z., 0009-0008-5139-7606; M.J.D.v.T., 0000-0003-1600-4279; R.G.M.B., 0000-0001-8151-1539; T.G., 0000-0002-3261-1186; A.C.L., 0000-0002-6703-2993; D.J.A.R.M., 0000-0003-3219-253X.

Correspondence: Federica R. Achini-Gutzwiller, Department of Hematology/Oncology/Immunology, Gene-Therapy, and Stem Cell Transplantation, University Children's Hospital Zurich–Eleonore Foundation & Children's Research Center, Steinwiesstrasse 75, 8032 Zurich, Switzerland; email: federica.achini-gutzwiller@hin.ch.

References

1. Waldmann H, Hale G. CAMPATH: from concept to clinic. *Philos Trans R Soc Lond B Biol Sci*. 2005;360(1461):1707-1711.
2. Lankester AC, Albert MH, Booth C, et al. EBMT/ESID inborn errors working party guidelines for hematopoietic stem cell transplantation for inborn errors of immunity. *Bone Marrow Transplant*. 2021;56(9):2052-2062.
3. Guilcher GMT, Shah R, Shenoy S. Principles of alemtuzumab immunoablation in hematopoietic cell transplantation for non-malignant diseases in children: a review. *Pediatr Transplant*. 2018;22(2):e13142.
4. Riechmann L, Clark M, Waldmann H, Winter G. Reshaping human antibodies for therapy. *Nature*. 1988;332(6162):323-327.
5. Buggins AG, Mufti GJ, Salisbury J, et al. Peripheral blood but not tissue dendritic cells express CD52 and are depleted by treatment with alemtuzumab. *Blood*. 2002;100(5):1715-1720.
6. Hale G. The CD52 antigen and development of the CAMPATH antibodies. *Cytotherapy*. 2001;3(3):137-143.
7. Clark M, Hale G, Waldmann H. Interaction of rat monoclonal antibodies with human killer cells. *Adv Exp Med Biol*. 1985;186:797-803.
8. Clark RA, Watanabe R, Teague JE, et al. Skin effector memory T cells do not recirculate and provide immune protection in alemtuzumab-treated CTCL patients. *Sci Transl Med*. 2012;4(117):117ra117.
9. Dyer MJ, Hale G, Marcus R, Waldmann H. Remission induction in patients with lymphoid malignancies using unconjugated CAMPATH-1 monoclonal antibodies. *Leuk Lymphoma*. 1990;2(3-4):179-193.
10. Hale G, Bright S, Chumbley G, et al. Removal of T cells from bone marrow for transplantation: a monoclonal antilymphocyte antibody that fixes human complement. *Blood*. 1983;62(4):873-882.
11. Hu Y, Turner MJ, Shields J, et al. Investigation of the mechanism of action of alemtuzumab in a human CD52 transgenic mouse model. *Immunology*. 2009;128(2):260-270.
12. Siders WM, Shields J, Garron C, et al. Involvement of neutrophils and natural killer cells in the anti-tumor activity of alemtuzumab in xenograft tumor models. *Leuk Lymphoma*. 2010;51(7):1293-1304.
13. Wiendl H, Kieseier B. Multiple sclerosis: reprogramming the immune repertoire with alemtuzumab in MS. *Nat Rev Neurol*. 2013;9(3):125-126.
14. Hotta R, Ohira M, Matsuura T, et al. CD52-negative NK cells are abundant in the liver and less susceptible to alemtuzumab treatment. *PLoS One*. 2016;11(8):e0161618.
15. Marsh RA, Lane A, Mehta PA, et al. Alemtuzumab levels impact acute GVHD, mixed chimerism, and lymphocyte recovery following alemtuzumab, fludarabine, and melphalan RIC HCT. *Blood*. 2016;127(4):503-512.
16. Marsh RA, Vaughn G, Kim MO, et al. Reduced-intensity conditioning significantly improves survival of patients with hemophagocytic lymphohistiocytosis undergoing allogeneic hematopoietic cell transplantation. *Blood*. 2010;116(26):5824-5831.
17. Chakrabarti S, MacDonald D, Hale G, et al. T-cell depletion with Campath-1H "in the bag" for matched related allogeneic peripheral blood stem cell transplantation is associated with reduced graft-versus-host disease, rapid immune constitution and improved survival. *Br J Haematol*. 2003;121(1):109-118.

18. Rebello P, Cwynarski K, Varughese M, Eades A, Apperley JF, Hale G. Pharmacokinetics of CAMPATH-1H in BMT patients. *Cytotherapy*. 2001;3(4):261-267.

19. Spyridonidis A, Liga M, Triantafyllou E, et al. Pharmacokinetics and clinical activity of very low-dose alemtuzumab in transplantation for acute leukemia. *Bone Marrow Transplant*. 2011;46(10):1363-1368.

20. Lane JP, Evans PT, Nademi Z, et al. Low-dose serotherapy improves early immune reconstitution after cord blood transplantation for primary immunodeficiencies. *Biol Blood Marrow Transplant*. 2014;20(2):243-249.

21. Admiraal R, Jol-van der Zijde CM, Furtado Silva JM, et al. Population pharmacokinetics of alemtuzumab (Campath) in pediatric hematopoietic cell transplantation: towards individualized dosing to improve outcome. *Clin Pharmacokinet*. 2019;58(12):1609-1620.

22. Dong M, Emoto C, Fukuda T, et al. Model-informed precision dosing for alemtuzumab in paediatric and young adult patients undergoing allogeneic haematopoietic cell transplantation. *Br J Clin Pharmacol*. 2022;88(1):248-259.

23. Achini-Gutzwiller FR, Jol-van der Zijde CM, Jansen-Hoogendijk AM, et al. Development and validation of an efficient and highly sensitive ELISA for alemtuzumab quantification in human serum and plasma. *Ther Drug Monit*. 2023;45(1):79-86.

24. Jonsson EN, Karlsson MO. Xpose–an S-PLUS based population pharmacokinetic/pharmacodynamic model building aid for NONMEM. *Comput Methods Programs Biomed*. 1999;58(1):51-64.

25. Lindbom L, Pihlgren P, Jonsson EN, Jonsson N. PsN-Toolkit–a collection of computer intensive statistical methods for non-linear mixed effect modeling using NONMEM. *Comput Methods Programs Biomed*. 2005;79(3):241-257.

26. Bergstrand M, Hooker AC, Wallin JE, Karlsson MO. Prediction-corrected visual predictive checks for diagnosing nonlinear mixed-effects models. *AAPS J*. 2011;13(2):143-151.

27. Keizer RJ, van Benten M, Beijnen JH, Schellens JH, Huitema AD. Piraña and PCluster: a modeling environment and cluster infrastructure for NONMEM. *Comput Methods Programs Biomed*. 2011;101(1):72-79.

28. R Core Team. R: A Language and Environment for Statistical Computing R Foundation for Statistical Computing. 2021. Accessed 5 June 2022. https://www.R-project.org/

29. RStudio Team. RStudio: Integrated Development for R. RStudio; 2020. Accessed 5 June 2022.

30. Willemsen L, Jol-van der Zijde CM, Admiraal R, et al. Impact of serotherapy on immune reconstitution and survival outcomes after stem cell transplantations in children: thymoglobulin versus alemtuzumab. *Biol Blood Marrow Transplant*. 2015;21(3):473-482.

31. Allen CE, Marsh R, Dawson P, et al. Reduced-intensity conditioning for hematopoietic cell transplant for HLH and primary immune deficiencies. *Blood*. 2018;132(13):1438-1451.

32. Wang Y, Jadhav PR, Lala M, Gobburu JV. Clarification on precision criteria to derive sample size when designing pediatric pharmacokinetic studies. *J Clin Pharmacol*. 2012;52(10):1601-1606.

33. Filipovich AH, Weisdorf D, Pavletic S, et al. National Institutes of Health consensus development project on criteria for clinical trials in chronic graft-versus-host disease: I. Diagnosis and staging working group report. *Biol Blood Marrow Transplant*. 2005;11(12):945-956.

34. Hale G, Rebello P, Brettman LR, et al. Blood concentrations of alemtuzumab and antiglobulin responses in patients with chronic lymphocytic leukemia following intravenous or subcutaneous routes of administration. *Blood*. 2004;104(4):948-955.

35. Arnold DE, Emoto C, Fukuda T, et al. A prospective pilot study of a novel alemtuzumab target concentration intervention strategy. *Bone Marrow Transplant*. 2021;56(12):3029-3031.

36. de Taeye SW, Bentlage AEH, Mebius MM, et al. FcγR binding and ADCC activity of human IgG allotypes. *Front Immunol*. 2020;11:740.

37. Temming AR, de Taeye SW, de Graaf EL, et al. Functional attributes of antibodies, effector cells, and target cells affecting NK cell-mediated antibody-dependent cellular cytotoxicity. *J Immunol*. 2019;203(12):3126-3135.

38. Admiraal R, van Kesteren C, Jol-van der Zijde CM, et al. Association between anti-thymocyte globulin exposure and CD4+ immune reconstitution in paediatric haemopoietic cell transplantation: a multicentre, retrospective pharmacodynamic cohort analysis. *Lancet Haematol*. 2015;2(5):e194-203.